

Transport of the δ -Opioid Receptor Agonist [*D*-Penicillamine^{2,5}] Enkephalin Across the Blood–Brain Barrier Involves Transcytosis¹

RICHARD D. EGLETON AND THOMAS P. DAVIS*

Contribution from *Department of Pharmacology, The University of Arizona, College of Medicine, LSN 533, 1501 N. Campbell Avenue, Tucson, Arizona 85724.*

Received October 14, 1998. Accepted for publication January 6, 1999.

Abstract □ The delta opioid receptor antagonist [*D*-penicillamine^{2,5}]-enkephalin (DPDPE) is an enzymatically stable peptide analogue of Met-enkephalin. DPDPE uses a saturable transport mechanism to cross the blood-brain barrier (BBB), though the exact mechanism is not fully understood. The aim of the present study was to identify the mechanism by which DPDPE enters the brain. The effect of phenylarsine oxide (PAO), an endocytosis inhibitor, on the transport of [³H]DPDPE was investigated using both in vitro and in situ transport studies. Two in vitro models of the BBB utilizing primary bovine brain microvascular endothelial cells (BBMEC) were studied. [³H]DPDPE permeability across monolayers of BBMEC grown on polycarbonate filters was studied. PAO significantly reduced the permeability of [³H]-DPDPE across the monolayer. PAO also reduced the uptake of [³H]-DPDPE into BBMEC cells, without affecting binding to the cells. The in situ perfusion model of the BBB was also studied, PAO reduced DPDPE uptake by the brain in a dose-dependent manner. These studies indicate that DPDPE enters the brain via an energy-dependent transcytotic mechanism.

Introduction

The blood-brain barrier (BBB), consisting of the cerebral capillary endothelial cells, restricts the entry of solutes into the brain. There are, however, a number of transport mechanisms that peptide drugs can utilize to enter the brain.² For example biphalin ([Tyr-*D*-Ala-Gly-Phe]₂), an enkephalin analogue, uses the large neutral amino acid transporter to enter the brain.³ The cyclic somatostatin analogue, CTAP (*D*-Phe-Cys-Tyr-*D*-Trp-Arg-Thr-Pen-Thr) enters the brain via a diffusional mechanism.⁴

[*D*-Penicillamine^{2,5}] enkephalin (DPDPE, Tyr-*D*-Pen-Gly-Phe-*D*-Pen) is a δ -opioid receptor agonist that is conformationally constrained by a disulfide bridge between the two *D*-Pen moieties.⁵ Conformationally constraining the peptide results in a higher enzymatic stability in both brain and serum^{6,7} compared with the endogenous enkephalins.⁸ In the bovine brain microvascular endothelial cell (BBMEC) model of the BBB, DPDPE had a higher permeability than most other opioid peptides studied.⁹

In situ perfusion studies have shown that DPDPE accumulates in the brain significantly better than the BBB-impermeable marker sucrose.¹⁰ This accumulation is partially saturable.¹⁰ The saturable component follows Michaelis–Menten kinetics with a maximum velocity (V_{max}) of $51.1 \pm 13.2 \text{ pmol} \cdot \text{min}^{-1} \cdot \text{g}^{-1}$, and a Michaelis–Menten constant (K_m) of $45.6 \pm 27.6 \text{ } \mu\text{M}$, and the nonsaturable component has a K_d of $0.6 \pm 0.3 \text{ } \mu\text{L} \cdot \text{min}^{-1} \cdot \text{g}^{-1}$.¹¹ Further studies show that DPDPE does not use a number of previously reported

peptide transporters, including the enkephalin transporter and the insulin transporter.¹¹ DPDPE uptake is also not dependent on any δ -opioid receptor-mediated mechanism.¹¹ Recent studies have shown an important role for endocytosis in the transport of peptides and proteins across the BBB,¹² and phenylarsine oxide (PAO) has been shown to inhibit saturable endocytotic mechanisms.¹³ In this study, we investigated the role of endocytosis in the transport of DPDPE in BBMEC monolayers and into the rat brain.

Experimental Procedures

In Vitro BBMEC Permeability Studies. BBMEC cells were isolated from the cerebral cortex gray matter as previously described.^{14,15} Isolated BBMECs, suspended in culture media, were seeded onto 25-mm polycarbonate membrane filters (Costar Nucleopore 10 μm ; Costar Corp., Cambridge, MA) that had previously been coated with rat-tail collagen and human fibronectin. After the cells had grown to confluence (10–12 days), the BBMEC monolayers were used for transendothelial transport studies of [³H]DPDPE in the presence and absence of PAO. The PAO was administered to both chambers commencing at the preincubation period.

Polycarbonate filters with confluent BBMEC monolayers were placed in side-by-side diffusion chambers (Crown Glass Company, Somerville, NJ) kept at 37 °C. Both sides of the diffusion cell chamber contained phosphate buffered saline (PBS) (122 mM NaCl, 3 mM KCl, 25 mM Na₂PO₄, 1.3 mM K₂HPO₄, 1.4 mM CaCl₂, 1.2 mM MgSO₄, 10 mM glucose, 10 mM HEPES pH 7.4) that was continuously stirred. At 15, 30, 60, 90, and 120 min, after the addition of 1 mL of [³H]DPDPE (0.33 $\mu\text{Ci} \cdot \text{mL}^{-1}$) to the donor chamber, 200 μL samples were removed from the receiver chamber. An equal volume of fresh PBS was added to the sampled chamber to maintain a constant volume during sampling. Four milliliters of Budget Solve Scintillation Cocktail (RPI, Mount Prospect, IL) was added to each sample, and the samples were counted for radioactivity using a Beckman Beta counter model LS 5000 TD (Fullerton, CA).

The effect of phenylarsine oxide on the basal permeability of the BBMEC membranes was studied using [¹⁴C]sucrose. [¹⁴C]-Sucrose has a very low permeability across BBMEC-coated membranes and is used to access basal permeability.

In Vitro BBMEC Uptake Studies. BBMEC cells were grown to confluence on 24 well plates (Falcon, Becton Dickinson, Lincoln Park, NJ) precoated with rat tail collagen and human fibronectin. Growth media was removed, and the cells were preincubated with assay buffer (122 mM NaCl, 3 mM KCl, 25 mM Na₂PO₄, 1.3 mM K₂HPO₄, 1.4 mM CaCl₂, 1.2 mM MgSO₄, 10 mM glucose, 10 mM HEPES pH 7.4). After 20 min, 0.33 μCi of [³H]DPDPE was added to each well. The cells were then incubated for 5–30 min at 37 °C on a shaker table. After the set time, the radioactive buffer was removed and the cells were washed three times with ice cold assay buffer and then incubated for 4 min with an acid buffer (0.2 M acetic acid in 0.2 M NaCl¹⁶). The acid wash was performed to strip any of the DPDPE from the external surface of the cell. Therefore, any radioactivity that remains with the cell has been taken into the cell itself. After 4 min, the acid wash was removed and the cells were incubated with a 1% Triton-X-100 for 30 min. Samples (100 μL) from both the acid wash and the Triton-X-100 wash were prepared for radioactive sampling by adding 4 mL of Budget Solve

* Corresponding author. Telephone: (520)-626-7643. Fax: (520)-626-4053. E-mail: davistp@u.arizona.edu.

Scintillation Cocktail to each sample, and the samples were counted for radioactivity using a Beckman Beta counter model LS 5000 TD (Fullerton, CA). The remaining samples were assayed for protein using a Pierce BCA-protein kit.

The effect of PAO on [³H]DPDPE uptake was studied at the 20-min time point. PAO (10–200 μM) was added to the cells during the preincubation and throughout the experimental time course. The experiment was repeated as already described.

In Situ Rat Brain Perfusion. The following experimental protocol was approved by the Institutional Animal Care and Use Committee at the University of Arizona. Adult Sprague–Dawley rats (weighing 250–350 g) were anesthetized with 1 mL·kg⁻¹ of a cocktail of acepromazine (0.6 mg·mL⁻¹), ketamine (3.1 mg·mL⁻¹), and xylazine (78.3 mg·mL⁻¹), and then heparinized (10 000 U·Kg⁻¹). The neck vessels were exposed, and the right common carotid artery was cannulated with fine silicon tubing connected to a perfusion system. The perfusion fluid was a modified Krebs-Henseleit Ringers¹⁷ [117.0 mM NaCl, 4.7 mM KCl, 0.8 mM MgSO₄·3H₂O, 24.8 mM NaHCO₃, 1.2 mM KH₂PO₄, 2.5 mM CaCl₂·6H₂O, 10 mM D-glucose, 39% dextran (MW 70 000), and 1% bovine serum albumin] that had been aerated with 5% CO₂, 95% O₂ and warmed to 37 °C. The right jugular vein was sectioned at the start of the perfusion. Once the correct perfusion pressure of 90.8 ± 5.3 mmHg and perfusion flow rate of 3.1 mL·min⁻¹ were obtained, the contralateral carotid artery was cannulated and perfused in the same manner. The [³H]DPDPE or [¹⁴C]sucrose, along with various concentrations of PAO (10–200 μM), 100 μM DPDPE, or 100 μM DPDPE + 100 μM PAO, was then infused via a slow-drive syringe pump (model 22, Harvard Apparatus, South Natick, MA) into the inflowing mammalian Ringers solution. After 20 min, the perfusion was terminated and the animals were sacrificed by decapitation. The brain was removed, choroid plexi were excised, and brain samples taken and weighed. Perfusion fluid samples were taken from the carotid cannulae immediately at the termination of the perfusion.

Brain tissue samples and 100 μL of perfusion fluid were prepared for liquid scintillation counting by 12 h of solubilization in 1 mL of tissue solubilizer (TS-2; Research Products, Mount Pleasant, IL). After solubilization, 100 μL of 30% acetic acid was added to each sample to eliminate chemiluminescence, followed by 4 mL of Budget Solve Scintillation Cocktail (Research Products). The samples were counted for radioactivity (model LS 5000 TD counter; Beckman Instruments, Fullerton, CA).

Materials. Radiolabeled Substances. [³H] Tyr¹ DPDPE (42 Ci·mmol⁻¹) was obtained from Chiron Mimotopes Peptide Systems (San Diego, CA), under the direction of the National Institute on Drug Abuse. [¹⁴C]Sucrose (672 mCi·mmol⁻¹) was purchased from NEN Research Products (Boston, MA).

Nonradiolabeled Substances. DPDPE was provided by Chiron Mimotopes Peptide Systems under the direction of the National Institute on Drug Abuse. PAO was purchased from Sigma (St. Louis, MO). All other chemicals were supplied by Sigma (St. Louis, MO) unless otherwise stated.

Expression of Results. In Vitro BBMEC Permeability. The flux of peptide was determined by the linear regression of picomoles of DPDPE appearing in the receiver chamber versus time in minutes. The apparent permeability constant (*PC*) was then calculated as

$$PC = \text{flux}/(AC_{D0}) \quad (1)$$

where flux is the gradient of the linear regression, *A* is the surface area of the membrane (0.636 cm²), and *C*_{D0} is the initial concentration in the donor chamber.

In Vitro BBMEC Uptake. The flux of peptide into the cells was determined by the linear regression of picomoles of DPDPE per milligram of protein associated with the cells versus time in minutes. The cell-associated radioactivity was composed of two components, the acid-sensitive (representing [³H]DPDPE bound to the cell surface) and the acid-insensitive uptake (representing the radioactivity within the cell).

In Situ Perfusion. The amount of radioactivity in the whole brain was expressed as the percentage ratio of the tissue concentration (*C*_{Tissue}, in dpm/g) to the concentration in the perfusion fluid (*C*_{Perf}, in dpm/mL).

$$R_{\text{Tissue}} (\%) = C_{\text{Tissue}}/C_{\text{Perf}} \times 100$$

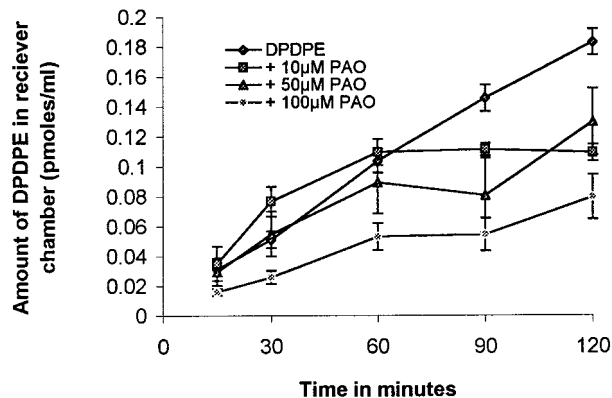


Figure 1—The permeability of [³H]DPDPE across BBMEC monolayers. Each point represents the mean and SEM of 12 individual BBMEC confluent monolayers on filters. Concentrations of phenylarsine oxide (PAO) from 10 to 100 μM led to significant inhibition of [³H]DPDPE permeability across the monolayers.

Table 1—Permeability Coefficient (*PC*) Values Calculated for [³H]DPDPE in the Presence of 10–100 μM PAO^a

PAO, μM	<i>PC</i> × 10 ⁻⁴ cm·min ⁻¹ (± SEM)	level of significance
0	9.31 (0.62)	—
10	3.73 (1.86)	<i>p</i> < 0.05
50	4.97 (1.24)	<i>p</i> < 0.05
100	3.54 (0.62)	<i>p</i> < 0.01

^a *PC* values calculated from Figure 1 were compared using ANOVA and Newman–Keuls analysis; there was no significant difference between the concentrations of PAO used.

Unidirectional rate constants, *K*_{in} (μL·min⁻¹g⁻¹) were determined by single time point analysis as described previously,¹⁸ where *T* is the time in minutes

$$K_{in} = C_{\text{Tissue}}(T)/C_{\text{perf}}T$$

The blood–brain unidirectional transfer constants determined in this manner were corrected for vascular space by subtracting the [¹⁴C]sucrose *R*_{Brain} from the [³H]DPDPE *R*_{Brain} values.

Statistical Analysis. For all experiments, the data were presented as the mean and SEM. All concentration effects of PAO on the [³H]DPDPE transport were compared by ANOVA, followed by Newman–Keuls using the Pharmacological Calculation System (PCS) statistical analysis program.¹⁹ Linear regressions were carried out using the PCS statistical analysis program, and compared by the method of Bailey.²⁰

Results

In Vitro BBMEC Permeability of [³H]DPDPE. The effect of PAO on the basal permeability of BBMEC monolayers to [¹⁴C]sucrose was studied. There was no effect on sucrose permeability across the membranes with 10, 50, or 100 μM PAO (data not shown). The permeability of [³H]DPDPE across BBMEC monolayers grown on collagen/fibronectin-coated polycarbonate filters and the effect of 10, 50, and 100 μM PAO were studied. Figure 1 shows the permeability of [³H]DPDPE with time. The *PC* values calculated from Figure 1 (Table 1) show that all concentrations of PAO led to a significant decrease in the rate of [³H]DPDPE permeability across the membrane. The amount of DPDPE in the receiver chamber was significantly lower at all time points in the presence of 100 μM PAO (*p* < 0.01 at all time points). Also, the values at 100 μM PAO were significantly lower than the values for 10 μM PAO for all but the 120-min time point (*p* < 0.05 for 10 and 90 min, *p* < 0.01 for 30 and 60 min). The 50 μM concentration of PAO significantly reduced DPDPE permeability at all time points studied (*p* < 0.05 at 15 and 60 min, *p* < 0.01 at 30,

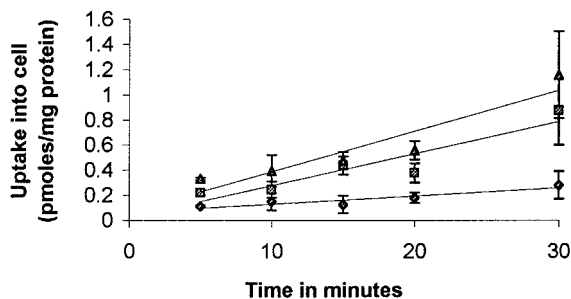


Figure 2—The time-dependent uptake of $[^3\text{H}]$ DPDPE into BBMEC monolayer cells. Each point represents the mean and SEM of eight wells. Triangles represent the total amount of DPDPE associated with the cells, and diamonds represent the acid-sensitive and squares represent the acid-insensitive fractions of the binding.

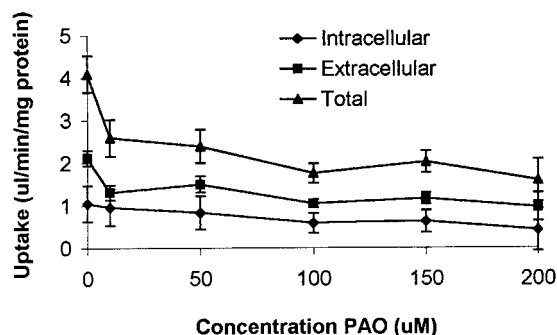


Figure 3—The effects of PAO (10–200 μM) on the total cell association of DPDPEs and acid-sensitive/acid-insensitive fractions at the 20-min time point. Each point represents the mean and SEM of eight wells.

60, and 90 min) and was significantly different from 10 μM PAO at the 30- and 60-min time points ($p < 0.01$ and $p < 0.05$, respectively). A solution 10 μM PAO reduced DPDPE permeability at the 90- and 120-min time point ($p < 0.05$ and $p < 0.01$, respectively).

In Vitro BBMEC Uptake of $[^3\text{H}]$ DPDPE. In the in vitro BBMEC model of the BBB, $[^3\text{H}]$ DPDPE uptake is linear with time with an uptake rate of $32.3 \pm 0.7 \text{ fmol}\cdot\text{min}^{-1}\cdot\text{mg}^{-1} \text{ protein}$ (Figure 2). The total uptake could be split into two components, the binding of $[^3\text{H}]$ DPDPE to the external membrane (acid sensitive), with a rate of $6.5 \pm 0.15 \text{ fmol}\cdot\text{min}^{-1}\cdot\text{mg}^{-1} \text{ protein}$; and the internalized fraction (acid insensitive), with a rate of $25.6 \pm 0.59 \text{ fmol}\cdot\text{min}^{-1}\cdot\text{mg}^{-1} \text{ protein}$. The uptake of $[^3\text{H}]$ DPDPE was significantly decreased at all concentrations of PAO (Figure 3). The acid-sensitive fraction showed no significant difference in $[^3\text{H}]$ DPDPE binding to the cell except at the 200- μM PAO concentration ($p < 0.05$), whereas the acid-insensitive uptake fraction was significantly reduced.

In Situ Perfusion. The effects of phenylarsine oxide concentrations ranging from 10 to 200 μM on the basal permeability of the BBB to $[^{14}\text{C}]$ sucrose were studied. PAO had no significant effect on the basal permeability of the BBB (Figure 4) at the concentrations used. All subsequent in situ figures have had the sucrose space subtracted.

The transport of $[^3\text{H}]$ DPDPE across the BBB was studied during in situ brain perfusion with various (10–200 μM) concentrations of PAO. Addition of PAO decreased the uptake of $[^3\text{H}]$ DPDPE into the rat brain in a dose-dependent manner (Figure 5, Table 2). The $[^3\text{H}]$ DPDPE uptake was decreased by 27% ($p < 0.05$) at 10 μM , 43% ($p < 0.01$) at 50 μM , 73% ($p < 0.01$) at 100 μM , 80% ($p < 0.01$) at 150 μM , and 49% ($p < 0.01$) at 200 μM PAO. The effects at both 100 and 150 μM were significantly different from those at 10 μM ($p < 0.05$ for both).

Addition of 100 μM nonradioactive DPDPE led to a significant inhibition of $[^3\text{H}]$ DPDPE uptake ($p < 0.01$)

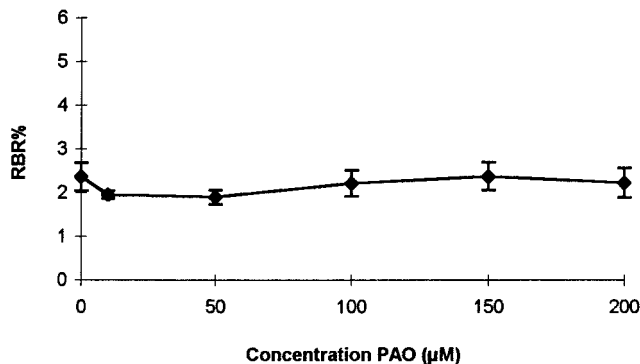


Figure 4—The effects of DPDPE and PAO on the permeability of the rat BBB to $[^{14}\text{C}]$ sucrose. Each bar represents the mean and SEM of 4–6 animals. Concentrations of 100 μM DPDPE and 100 μM PAO had no significant effect on the permeability of the BBB to sucrose.

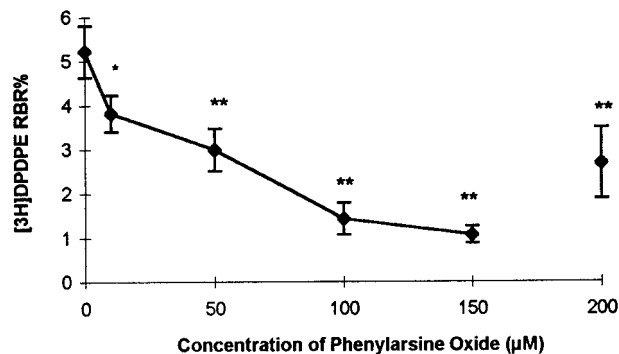


Figure 5—Dose-dependent inhibition of $[^3\text{H}]$ DPDPE in situ uptake by rat brains of 10–200 μM PAO. Each point represents the mean and SEM of 4–6 animals. Statistical significance is indicated by (*) $p < 0.05$ and (**) $p < 0.01$ (using ANOVA followed by Newman–Keuls ad hoc test with the sucrose space subtracted).

Table 2—Unidirectional Transfer Constants (K_{in}) for $[^3\text{H}]$ DPDPE in the Presence of Various Concentrations of PAO^a

PAO, μM	K_{in} ($\mu\text{L}\cdot\text{min}^{-1}\cdot\text{g}^{-1}$) \pm SEM	percent change (p value)
0	2.61 ± 0.29	—
10	1.91 ± 0.21	27% ($p < 0.05$)
50	1.49 ± 0.27	43% ($p < 0.01$)
100	0.71 ± 0.17	73% ($p < 0.01$) ^b
150	0.53 ± 0.10	80% ($p < 0.01$) ^b
200	1.30 ± 0.39	51% ($p < 0.05$)

^a The unidirectional transport constants (K_{in}) for $[^3\text{H}]$ DPDPE calculated from Figure 5 and the percent decrease in the constants with 10–200 μM PAO. Concentrations of PAO from 50 to 200 μM led to significant decreases in the K_{in} values (K_{in} values compared by ANOVA, followed by Newman–Keuls test).
^b This value is also significantly different from 10 μM PAO data at $p < 0.05$.

(Figure 6). Co-administration of both PAO and cold DPDPE led to no additive inhibition of $[^3\text{H}]$ DPDPE uptake.

Discussion

In this study, we investigated the role of a saturable endocytotic mechanism in the transport of DPDPE (a cyclized opioid peptide) into the brain, using a three-model BBB paradigm. It is assumed with each of the three models that the receiver chamber, cells, or brain are acting as a sink (i.e., that the transport of DPDPE will be in one direction only). We also assume that the transport will be linear. The concentration of peptide that we used in this study is 7.6 pM. This concentration is considerably lower than the half-saturation constant of the peptide transporter, which is 45.5 μM .¹¹ Thus, the concentration we use

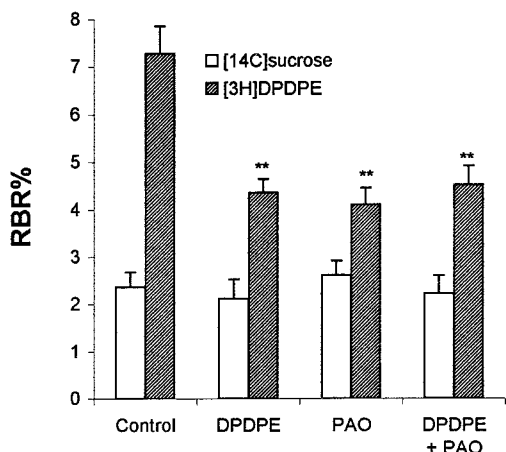


Figure 6—The effects of a combination of 100 μM PAO and 100 μM DPDPE on the uptake of $[^3\text{H}]\text{DPDPE}$ by rat brain. Each bar represents the mean and SEM of 4–6 animals. Addition of PAO, DPDPE, and the combination to the perfusate led to a significant decrease in $[^3\text{H}]\text{DPDPE}$ uptake. There was no significant difference between the three treatment groups.

is 10^{-6} lower than the concentration required to saturate the transport. This concentration is thus reasonable and we assume that the sink conditions will occur, if the amount of peptide in the donor solution remains higher than the amount of peptide in the receiver chamber. In this study, only a small percentage of the peptide actually crosses into the receiver chamber, cell, or brain. If the concentration of peptide used in a study is lower than the K_m value, it is likely that the process will remain linear.

The trivalent monosubstituted organoarsenic compound, PAO has been shown to inhibit endocytosis via clathrin coated pits²¹ and has been used to study receptor-mediated endocytosis at concentrations of 0.1 to 100 μM .¹⁶ The major toxic effect of PAO is the inhibition of cellular pyruvate dehydrogenase, which results in a decrease in ATP production via the citric acid cycle.²² Viability of MDCK cells in the presence of PAO was maintained in the presence of 5 mM glucose.²² In all of our models, of the BBB the concentration of glucose was 10 mM. Most of the other toxic effects of PAO are generally seen at longer time points than those used in this study and can be related to its long-term inhibition of endocytosis.

The first model of the BBB that was investigated in the present study was the *in vitro* permeability of $[^3\text{H}]\text{DPDPE}$ across BBMEC monolayers. In general, this model of the BBB is used to study the transport of nonradioactive peptides across the BBB, and the typical concentrations used (i.e., 500 μM) will result in the predominant mode of transport being diffusion. In this report, we used $[^3\text{H}]\text{DPDPE}$ with a specific activity of 42 Ci·mM⁻¹, and 0.33 μCi was added to each of the donor chambers (i.e., approximately 7.6 pM compared with 500 μM of peptide added in cold experiments). This low pmolar concentration of $[^3\text{H}]\text{DPDPE}$ is similar to that used in the *in situ* model and thus makes comparison easier. If we assume a cerebrovascular surface area of 100 cm²·g⁻¹,²³ the permeability surface area constant (PC) for the *in situ* $[^3\text{H}]\text{DPDPE}$ is $1.46 \pm 0.31 \text{ cm}\cdot\text{min}^{-1} \times 10^{-5}$ compared with a cold 500 μM *in vitro* value of $49.24 \pm 2.78 \text{ cm}\cdot\text{min}^{-1} \times 10^{-4}$.⁹ This result is a 337-fold difference. In contrast, when the *in vitro* study is carried out with $[^3\text{H}]\text{DPDPE}$, the PC value is $9.31 \pm 0.62 \text{ cm}\cdot\text{min}^{-1} \times 10^{-4}$, which is a 64-fold difference. From the previous *in situ* studies^{10,11} it is known that the K_m for DPDPE is $45.6 \pm 27.6 \mu\text{M}$. Therefore, in the control DPDPE permeability studies, any transport system expressed by the cells would be thoroughly saturated at the 500 μM concentration. However, in the present study, the $[^3\text{H}]\text{DPDPE}$ is at a concentration of 7.6 pM, which would not

saturate the transporters. Therefore, it is likely that a larger proportion of the permeability across the membranes is due to a transport mechanism other than diffusion. Previous studies have used this model to study the transport of insulin²⁴ and angiotensin II.¹³ These peptides are biologically important and use receptor-mediated transcytosis to enter the brain. Furthermore, both of these previous studies used concentrations of PAO similar to those used in this study, and neither group reported any adverse effects of PAO on the membranes or cells studied. In the present study, PAO led to a significant decrease in the permeability of DPDPE across BBMEC monolayers (Figure 1). The basal permeability of the monolayers to $[^{14}\text{C}]\text{sucrose}$ was not effected by PAO (data not shown), indicating that the monolayer was not adversely affected by the PAO. In previous studies, it has been shown that the presence of high glucose will protect cell viability against PAO,²² and 10 mM glucose was used in these experiments. The higher concentration of PAO (100 μM) led to an inhibition at all time points of DPDPE permeability. There was a dose-dependent effect on the inhibition between the 10 and 100 μM concentrations. The 10 μM concentration significantly inhibited the permeability of $[^3\text{H}]\text{DPDPE}$ only at 90 and 120 min. The $[^3\text{H}]\text{DPDPE}$ (7.6 pM) permeability in the presence of 100 μM PAO was significantly different from the 10 μM PAO concentration at all time points except the 120-min time point.

The uptake of $[^3\text{H}]\text{DPDPE}$ into confluent monolayers of BBMEC cells was also studied. The uptake of DPDPE by the cells was linear with time (Figure 2). To assess the actual uptake into the cell, an acid wash was carried out. The peptide that was acid sensitive represented the amount of peptide bound to the outer membrane of the cells. The acid-sensitive fraction remained fairly consistent throughout the time-course of the uptake, with no significant difference in binding to the cells at any time point. PAO has been shown to cross-link vicinal sulfhydryl groups to form stable ring structures, thus inhibiting the internalization of receptors.²⁵ However, it is also possible that PAO could be preventing DPDPE from binding to sites on the membrane responsible for its uptake. PAO (10–200 μM) significantly reduced the uptake of $[^3\text{H}]\text{DPDPE}$ (Figure 3), without affecting the acid-sensitive portion (except at 200 μM). Thus it is evident that PAO was preventing internalization rather than cell surface binding of the DPDPE. Similar results have been seen with other peptides, such as angiotensin II in rat myometrial cells²⁶ and BBMEC.¹³

For both of the *in vitro* models of the BBB, the cells were grown without co-culture with astrocytes or astrocyte-conditioned media. A number of groups have reported improved BBB characteristics due to addition of either astrocytes or media from astrocytes.^{27,28} However, in studies carried out in this laboratory, we have found no significant change in either trans-endothelial resistance or sucrose crossing of monolayers due to either astrocyte-conditioned media or co-culture.²⁹ In fact, our sucrose space and trans-endothelial resistance measurements indicate that we have a tighter *in vitro* BBB than those reported by other groups who use co-culture.^{27,28}

The *in situ* perfusion model used in this study has been previously utilized to study the transport of a number of peptide neuropharmaceuticals across the BBB.^{3,4,10,30} The basal permeability of the BBB has been extensively studied using inert nontransported substances such as sucrose. In this study, the sucrose space was measured to assess the effect of PAO on the basal permeability of the BBB. The values measured ranged from 0.12 ± 0.002 to $0.13 \pm 0.002 \mu\text{L}\cdot\text{min}^{-1}\cdot\text{g}^{-1}$ for basal and PAO-treated rats, respectively. These values are well within the range of normal sucrose spaces reported previously in the literature.^{31,17,10} It is thus

Table 3—Comparison of *PC* Values from Literature and Those Calculated from This Study for DPDPE

model of BBB	<i>PC</i> , cm·min ⁻¹	reference
BBMEC permeability with 500 μM DPDPE	49.24 × 10 ⁻⁴	Weber et al., 1993
BBMEC permeability with [³ H]DPDPE	9.31 × 10 ⁻⁴	present study
in situ with [³ H]DPDPE	1.46 × 10 ⁻⁵	Williams et al., 1996
uptake studies with [³ H]DPDPE	2.61 × 10 ⁻⁵	present study
	9.56 × 10 ⁻⁵	present study

clear that, within the experimental parameters studied, PAO has no significant effect on the basal permeability of the BBB for a 20-min exposure. Furthermore, 100 μM DPDPE did not significantly affect the vascular space under the current experimental conditions. The uptake of DPDPE was inhibited in a dose-dependent manner by 10–150 μM PAO (Figure 5.). The inhibition caused by 100 μM PAO was not significantly different from that caused by 100 μM DPDPE, and no additive effect was observed on co-administration (Figure 6). At the 200 μM concentration of PAO, there was a slight yet not statistically significant rise in the uptake of DPDPE into rat brains. This rise was obviously not due to an increased basal permeability of the BBB because at the same concentration there was no increase in the sucrose space of the brain. Furthermore, a similar effect was not seen in the cellular uptake model.

PAO has been shown to have similar effects on the uptake/transport of DPDPE in two in vitro and one in situ model of BBB transport. It is generally difficult to compare in vivo and in vitro studies of the BBB. However, in this study, all the chemicals used were similar and the isotope was from the same batch and equivalent concentrations of isotope were used in each experiment. To make comparison of the three models easier, the flux and *K_{in}* values were converted to a *PC* value that was already described for the in situ experiments. The *PC* values for the uptake were calculated on the assumption that the mean protein value was 59.6 μg of protein per well (based on 162 individual wells) and the surface area of the wells is fixed at 2 cm². The *PC* values from this study and others (Table 3.) show that the BBMEC uptake studies have *PC* values 3.6 times higher than the in situ studies.

PAO has been used at concentrations ranging from 1 to 100 μM in a number previous studies and has resulted in variable levels of inhibition on receptor-mediated endocytosis. For example, Bradley et al.³² showed that the receptor-mediated endocytosis of low-density lipoprotein by human umbilical vein endothelial cells was reduced 66% by 1 μM PAO. Wiley et al.¹⁶ used a range of PAO concentrations (10⁻⁴–10⁻⁷ M) to inhibit receptor-mediated endocytosis of EGF by human fibroblast cells, finding that there was almost total inhibition at 10 μM. In contrast, angiotensin II receptor-mediated transcytosis across endothelial cells was significantly decreased by 25 μM PAO, though it required 100 μM PAO to significantly reduce uptake into the cell.¹³ These differences in the required concentrations of PAO to cause an effect may be linked to the differences in the endocytotic rate constants for each receptor studied and to the number of receptors expressed in a given system. For example, EGF receptors have endocytotic rate constants ranging from 0.03 to 0.3 min⁻¹, depending on cell type.³³ Also, receptor distribution and density varies from cell type to cell type, for example, the transferrin receptor is constitutively expressed at a high density on the BBB endothelial cells and relatively low in other capillary beds.³⁴ The fact that we were unable to totally inhibit the permeability across BBMEC cells on filters is not surprising. The *PC* value takes into account

the diffusion across the membranes between cells (by calculating the *PC* value from linear regression), however, it does not divide the transport into saturable and nonsaturable mechanisms. The evidence that we present in this study is that the saturable component of DPDPE transport is inhibited by PAO, thus implicating clathrin-dependent receptor-mediated endocytosis. It has been shown that DPDPE also uses a nonsaturable diffusional mechanism to cross the BBB.¹¹ This mechanism would not be affected by PAO and thus should not be inhibited. Therefore, we would be more surprised if we totally inhibited all DPDPE transport.

Together with data from previous studies, we can now state that DPDPE crosses the BBB in part via an endocytotic (transport) mechanism. PAO has been shown to inhibit some fluid phase endocytosis²⁵ at higher concentrations. Although this form of endocytosis may explain some of the DPDPE transport, it would not explain the saturable component of the transport. Furthermore, if the PAO were indeed inhibiting the nonsaturable component of the transport, it would be reasonable to assume that addition of a high concentration of DPDPE to the in situ media would lead to an additive inhibition. This assumption is evidently not the case (Figure 6), and the likely saturable mechanism is endocytosis. The two saturable forms of endocytosis are adsorptive endocytosis and receptor-mediated endocytosis. In an earlier study, the competitive adsorptive endocytosis inhibitor poly-L-lysine failed to reduce DPDPE uptake into rat brain,¹¹ suggesting that DPDPE does not bind to the anion-rich sites in the cell membrane and thus does not use classical adsorptive endocytosis. DPDPE has been shown to have a *K_m* in the micromolar range,¹¹ which is indicative of a carrier-mediated rather than receptor-mediated process.³⁵ This result would indicate that the mechanism of DPDPE uptake is unlikely to be via a normal receptor-mediated endocytotic effect. However, DPDPE transport could be explained by DPDPE binding specifically to a protein/receptor in an area that has a high basal endocytotic rate (for example, clathrin-coated pits) and entering the cell via receptor turnover rather than stimulating its own endocytosis. PAO has previously been shown to reduce the basal endocytotic rate in 3T3 cells²⁵ and could inhibit DPDPE uptake in this manner. Furthermore, insulin, which binds to its receptor (in clathrin-coated pits) and is internalized, leads to an increase in the basal endocytotic rate and also increases DPDPE uptake.¹¹

In conclusion, the present study demonstrates that DPDPE enters the brain via an endocytotic mechanism that is saturable and can be inhibited in a dose-dependent fashion by PAO. The understanding of the transport of DPDPE is important for several reasons. First, a number of opioid peptides based on the structure of DPDPE are currently being developed and studied for analgesia therapy. Second, the disulfide bridge between two D-amino acids has become a common strategy for stabilizing the peptide backbone of peptide pharmaceuticals. By studying the transport of DPDPE, we will be able to determine whether cyclization via disulfide bridges results in a common transport mechanism for peptide drugs.

References and Notes

1. This work was supported by NIDA grants no. DA-06284 and RO1-DA-11271.
2. Egleton, R. D.; Davis, T. P. Bioavailability and transport of peptides and peptide drugs into the brain. *Peptides* **1997**, *18*, 1431–1439.
3. Abbruscato, T. J.; Thomas, S. A.; Hruby, V. J.; Davis, T. P. Brain and spinal cord distribution of biphalin: Correlation

- with opioid receptor density and mechanism of CNS entry. *J. Neurochem.* **1997**, *69*, 1236–1245.
4. Abbruscato, T. J.; Thomas, S. A.; Hruby, V. J.; Davis, T. P. Blood-brain barrier permeability and bioavailability of a highly potent and μ -selective opioid receptor antagonist, CTAP: Comparison with morphine. *J. Pharm. Exp. Ther.* **1997**, *280*, 402–409.
 5. Mosberg, H. I.; Hurst, R.; Hruby, V. J., Gee, K.; Yamamura, H. I.; Galligan, J. J.; Burks, T. F. Bis-penicillamine enkephalins possess highly improved specificity toward delta opioid receptors. *Proc. Natl. Acad. Sci., U.S.A.* **1983**, *80*, 5871–5874.
 6. Weber, S. J.; Greene, D. L.; Sharma, S. D.; Yamamura, H. I.; Kramer, T. H.; Burks, T. F.; Hruby, V. J.; Hersh, L. B.; Davis, T. P. Distribution and analgesia of [3H][D-Pen2, D-Pen5] enkephalin and two halogenated analogues after intravenous administration. *J. Pharm. Exp. Ther.* **1991**, *259*, 1109–1117.
 7. Weber, S. J.; Greene, D. L.; Hruby, V. J.; Yamamura, H. I.; Porreca, F.; Davis, T. P. Whole body and brain distribution of [3H]cyclic[D-Pen2, D-Pen5] enkephalin after intraperitoneal, intravenous, oral and subcutaneous administration. *J. Pharm. Exp. Ther.* **1992**, *263*, 1308–1316.
 8. Dupont, A.; Cusan, L.; Garon, M.; Alvarado-Urbina, G.; Labrie, F. Extremely rapid degradation of [3H] methionine-enkephalin by various rat tissues in vivo and in vitro. *Life Sci.* **1977**, *21*, 907–914.
 9. Weber, S. J.; Abbruscato, T. J.; Brownson, E. A.; Lipkowski, A. W.; Polt, P.; Misicka, A.; Haaseth, R. C.; Bartosz, H.; Hruby, V. J.; Davis, T. P. Assessment of an in vitro blood-brain barrier model using several [Met5]enkephalin opioid analogues. *J. Pharm. Exp. Ther.* **1993**, *266*, 1649–1655.
 10. Williams, S. A.; Abbruscato, T. J.; Hruby, V. J.; Davis, T. P. Permeability of a δ -opioid receptor selective methionine-[D-penicillamine2,5]enkephalin, across the blood-brain and blood-cerebrospinal fluid barriers. *J. Neurochem.* **1996**, *66*, 1289–1299.
 11. Thomas, S. A.; Abbruscato, T. J.; Hruby, V. J.; Davis, T. P. The entry of [D-penicillamine2,5]enkephalin into the central nervous system: saturation kinetics and specificity. *J. Pharm. Exp. Ther.* **1997**, *280*, 1235–1240.
 12. Tamai, I.; Sai, Y.; Kobayashi, H.; Kamata, M.; Wakamiya, T.; Tsuji, A. Structure-internalization relationship for adsorptive-mediated endocytosis of basic peptides at the blood-brain barrier. *J. Pharmacol. Exp. Ther.* **1997**, *280*, 410–415.
 13. Rose, J. M.; Audus, K. L. Receptor-mediated angiotensin II transcytosis by brain microvessel endothelial cells. *Peptides* **1998**, *19*, 1023–1030.
 14. Audus, K. L.; Borchardt, R. T. Characterization of an in vitro blood-brain barrier model system for studying drug transport and metabolism. *Pharm. Res.* **1986**, *3*, 81–87.
 15. Audus, K. L.; Borchardt R. T. Bovine brain microvessel endothelial cell monolayers as a model system for the blood-brain barrier. *Ann. N. Y. Acad. Sci.* **1987**, *507*, 9–18.
 16. Wiley, H. S.; Cunningham, D. D. A cellular parameter for quantitating receptor mediated endocytosis. *J. Biol. Chem.* **1982**, *257*, 4222–4229.
 17. Preston, J. E.; Al-Sarraf, H.; Segal, M. B. Permeability of the developing blood-brain barrier to 14C-mannitol using the rat in situ brain perfusion technique. *Dev. Brain Res.* **1995**, *87*, 69–76.
 18. Zlokovic, B. V.; Begley, D. J.; Djuricic, B. M.; Mitrovic, D. M. Measurement of solute transport across the blood-brain barrier in the perfused guinea-pig brain: Method and application to *N*-methylaminoisobutyric acid. *J. Neurochem.* **1986**, *46*, 1444–1451.
 19. Tallarida, R. J.; Murray, B. M. *Analysis of Variance. Manual of Pharmacologic Calculations with Computer Programs*, 2nd ed.; Springer-Verlag: New York, 1987; pp 110–124.
 20. Bailey, N. T. J. *Regression Analysis. Statistical Methods in Biology*; English University Press: London, 1959; pp 91–99.
 21. Roosterman, D.; Roth, A.; Kreienkamp, H. J.; Richter, D.; Meyerhof, W. Distinct agonist-mediated endocytosis of cloned rat somatostatin receptor expressed in insulinoma cells. *J. Neuroendocrinol.* **1997**, *9*, 741–751.
 22. Liebl, B.; Muckter, H.; Doklea, E.; Reichl, F. X.; Fichtl, B.; Forth, W. Influence of glucose on the toxicity of oxophenylarsine in MDCK cells. *Arch. Toxicol.* **1995**, *69*, 421–424.
 23. Pardridge, W. M.; Triguero, D.; Yang, J. P. A. Comparisons of in vitro and in vivo models of transcytosis through the blood-brain barrier. *J. Pharm. Exp. Ther.* **1990**, *253*, 884–891.
 24. Miller, D. W.; Keller, B. T.; Borchardt, R. T. Identification and distribution of insulin receptors on cultured bovine brain microvessel endothelial cells: Possible function in insulin processing in the blood-brain barrier. *J. Cell Physiol.* **1994**, *161*, 333–341.
 25. Frost, S. C.; Lane, M. D.; Gibbs, E. M. Effect of phenylarsine oxide on fluid phase endocytosis: Further evidence for activation of the glucose transporter. *J. Cell. Physiol.* **1989**, *141*, 464–474.
 26. Lazari, M. F.; Porto, C. S.; Freymuller, E.; Abreu, L. C.; Picarelli, Z. P. Receptor-mediated endocytosis of angiotensin II in rat myometrial cells. *Biochem. Pharmacol.* **1997**, *54*, 399–408.
 27. Dehouck, M. P.; Jolliet-Riant, P.; Bree, F.; Fruchart, J. C.; Cecchelli, R.; Tillement, J. P. Drug transfer across the blood-brain barrier: Correlation between in vitro and in vivo models. *J. Neurochem.* **1992**, *58*, 1790–1797.
 28. Raub, T. J.; Kneutzel, S. I.; Sawada, G. A. Barrier tightening by a factor released from astroglia cells. *Exp. Cell. Res.* **1992**, *199*, 330–340.
 29. Abbruscato, T. J.; Davis, T. P. Combination of hypoxia/aglycemia compromises blood-brain barrier integrity. *J. Pharm. Exp. Ther.*, in press.
 30. Egleton, R. D.; Abbruscato, T. J.; Thomas, S. A.; Davis, T. P. Transport of opioid peptides into the central nervous system. *J. Pharm. Sci.* **1998**, *87*, 1433–1439.
 31. Zlokovic, B. V.; Banks, W. A.; Kadi, H. E.; Erchegeyi, J.; Mackic, J. B.; McComb, J. G.; Kastin, A. J. Transport, uptake and metabolism of blood-borne vasopressin by the blood-brain barrier. *Brain Res.* **1992**, *590*, 213–218.
 32. Bradley, J. R.; Johnson, D. R.; Pober, J. S. Four different classes of inhibitors of receptor mediated endocytosis decrease tumour necrosis factor-induced gene expression in human endothelial cells. *J. Immunol.* **1993**, *150*, 5544–5555.
 33. Koenig, J. A.; Edwardson, J. M. Endocytosis and recycling of G protein-coupled receptors. *Trends Pharmacol. Sci.* **1997**, *18*, 276–287.
 34. Jefferies, W. A.; Brandon, M. R.; Hunt, S. V.; Williams, A. F.; Gatter, K. C.; Mason, D. Y. Transferrin receptor on the endothelium of brain capillaries. *Nature* **1984**, *312*, 162–163.
 35. Zlokovic, B. V.; Hyman, S.; McComb, J. G.; Lipovac, M. N.; Tang, G.; Davson, H. Kinetics of arginine-vasopressin uptake at the blood-brain barrier. *Biochim. Biophys. Acta* **1990**, *1025*, 191–198.

JS980410+